Title

Bond Graph Modeling of a Planar Vehicle with Electric Traction Motors for Assisted Torque-Vectoring

Journal

2021 International Conference on Bond Graph Modeling and Simulation, ICBGM 2021, 53(3)

ISSN

07359276

Authors

Lee, Donghun
Loyola, Jonathan
McCrone, Jordan
et al.

Publication Date

2021

Peer reviewed

BOND GRAPH MODELING OF A PLANAR VEHICLE WITH ELECTRIC TRACTION MOTORS FOR ASSISTED TORQUE-VECTORING

Donghun Lee
Hyundai Motor Company, Hwaseong-si, Gyeonggi-do, 18280, Rep. of Korea,
a.dhoonil@hyundai.com

Jonathan Loyola
Jordan McCrone
Donald L. Margolis
Department of Mechanical Engineering and Aerospace Engineering,
University of California, Davis, Davis, California, 95616, USA
jonloyola@ucdavis.edu, djmccrone@ucdavis.edu, dlmargolis@ucdavis.edu

ABSTRACT

Powertrains for vehicles are transitioning from the internal combustion engine to electric motors. Electric motors have the ability to both output traction and generative braking torque. Furthermore, electric motor powertrains have a smaller size compared to the internal combustion engine powertrain. This opens up the possibility of different configurations of powertrain layouts. This paper explores an electric vehicle model with motors on both the front and the rear axles. The planar vehicle model with varying motor torque distribution is simulated to validate its handling dynamics.

Keywords: vehicle dynamics, electric vehicle, torque distribution.

1 INTRODUCTION

With environmental concerns becoming more and more important, the automobile industry has invested in vehicles that use an electric powertrain. The electric vehicle(EV) has a smaller powertrain size compared to the internal combustion engine. Additionally, regenerative torque from the electric motor can be used as a braking torque. Vehicle manufacturers test different powertrain layouts with these advantages. Many researchers suggest the in-wheel motor system and study the advantages of that system on handling performance(Osborn, Russell P., and Taehyun Shim 2006; De Novellis et al. 2013). However, the in-wheel motor system has restrictions and disadvantages in a mass-produced vehicle. Therefore, a two-traction motor system is adapted by vehicle makers in an all-wheel drive design(De Novellis et al. 2013). This two-traction motor system is similar to existing all-wheel drive systems. However, the two-traction motor system has its own advantage, where the motors can be controlled independently. This paper establishes a planar vehicle model and simulates a handling maneuver to demonstrate the advantages of the two-traction motor system.

ICBGM'2021 Nov 8-10, 2021- San Diego, California USA - ©2021 Society for Modeling & Simulation International (SCS)

2 MODELING OF THE PLANAR VEHICLE

2.1 Schematic of the planar vehicle

There are many all-wheel drive systems that can be used. In this paper, an all-wheel drive system which has two traction motors is studied. One motor is located on each of the front and rear axles. This electric power train layout allows independent traction torque control for each axle. Figure 1 shows a schematic of a powertrain layout for an electric vehicle.

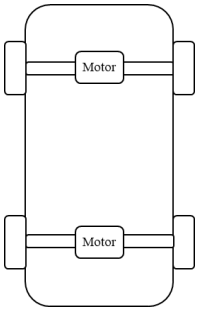

Figure 1: Powertrain layout of electric vehicle for AWD.

A planar vehicle model has three body degrees-of-freedom; longitudinal, lateral and rotational yaw motion. The model has 4 tires, each generating longitudinal and lateral forces. The vehicle has a steering angle as the input on the front wheels. Figure 2 and figure 3 show velocity and force diagrams for the planar vehicle model, respectively.

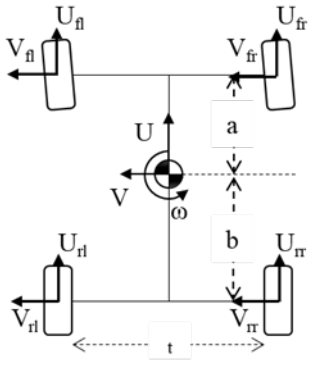

Figure 2: Velocity diagram of planar vehicle model

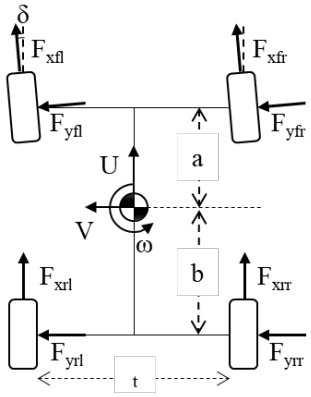

Figure 3: Force diagram of planar vehicle model.

The vehicle parameters are described in the appendix. In figure 2, U is the longitudinal velocity, V is the lateral velocity V and ω is the yaw rate. The longitudinal and the lateral velocity of each tire, as well as the longitudinal and the lateral acceleration of the vehicle are derived with body fixed coordinate.

$$U_{fl} = U_{rl} = U - \frac{t}{2}\omega$$

$$U_{fr} = U_{rr} = U + \frac{t}{2}\omega$$

$$V_{fl} = V_{fr} = V + a\omega$$

$$V_{rl} = V_{rr} = V - b\omega$$

$$a_x = \dot{U} - \omega V$$

$$a_y = \dot{V} + \omega U$$

2.2 Wheel and tire dynamics

Each tire has its own wheel dynamics that yields the rotational speed of the wheel ω_w. Figure 4 shows a schematic of the wheel.

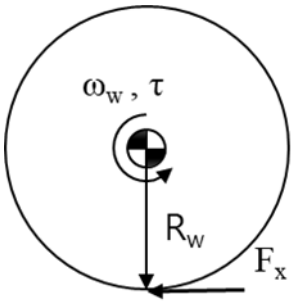

Figure 4: Schematic of wheel dynamics

$$J_w\dot{\omega}_w = \tau - R_w F_x$$

The input torque (τ) comes from the traction motor. The motor torque is applied to both wheels equally. Each wheel speed is independent.

This paper uses the Dugoff Tire Model(Dugoff et al. 1970) for the tire force calculation which uses the slip ratio of the tire s_x and the side slip angle of the tire α. μ is the friction of the surface (μ≤1)

$$F_x = f(\mu, N, s_x, C_x)$$

$$s_{xij} = \frac{R_W\omega_{wij} - U_{ij}}{|U_{ij}|},$$

$$i = front, rear, j = left, right$$

$$F_y = f(\mu, N, \alpha, C_\alpha)$$

$$\alpha_{fj} = \delta - \frac{V_{fj}}{U_{fj}}, \qquad j = left, right$$

$$\alpha_{rj} = \frac{V_{rj}}{U_{rj}}, \qquad j = left, right$$

The steering angle (δ) is considered to be very small, such that small angle approximations are valid.

The Dugoff Tire Model requires the normal force N of each tire. The normal force of each tire is calculated with the acceleration and the roll stiffness of the vehicle (k_{rf}, k_{rr}) (Dugoff et al. 1970; Margolis, Donald L., and Jahan Asgari 1991). The normal force of each wheel is derived with assuming a quasi-static load transfer condition.

$$N_{fl} = \frac{b}{2(a+b)}Mg - \frac{k_{rf}}{t(k_{rf}+k_{rr})}Mh_{cg}a_y - \frac{1}{2(a+b)}Mh_{cg}a_x$$

$$N_{fr} = \frac{b}{2(a+b)}Mg + \frac{k_{rf}}{t(k_{rf}+k_{rr})}Mh_{cg}a_y - \frac{1}{2(a+b)}Mh_{cg}a_x$$

$$N_{rl} = \frac{a}{2(a+b)}Mg - \frac{k_{rr}}{t(k_{rf}+k_{rr})}Mh_{cg}a_y + \frac{1}{2(a+b)}Mh_{cg}a_x$$

$$N_{rr} = \frac{a}{2(a+b)}Mg + \frac{k_{rr}}{t(k_{rf}+k_{rr})}Mh_{cg}a_y + \frac{1}{2(a+b)}Mh_{cg}a_x$$

The tire lateral force increases as side slip angle is increased. However, the maximum force of tire cannot exceed μ_N. Therefore, a lateral force is saturated at some point. Figure 5 shows the lateral tire force-side slip angle for varying F_x values while maintaining the same normal force using the Dugoff Tire Model.

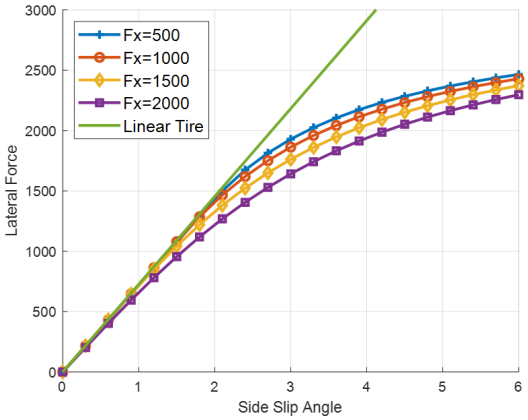

Figure 5: Lateral tire force of Dugoff's tire model

The lateral force in the Dugoff Tire Model has linear characteristic with small side slip angle. However, it displays a non-linear behavior as side slip angle is increased. this non-linearity makes different vehicle motion with respect to F_x in the same longitudinal velocity and steering input.

2.3 Bond graph for vehicle model

The bond graph with all the above dynamic equations and tire model is presented in Figure 6.

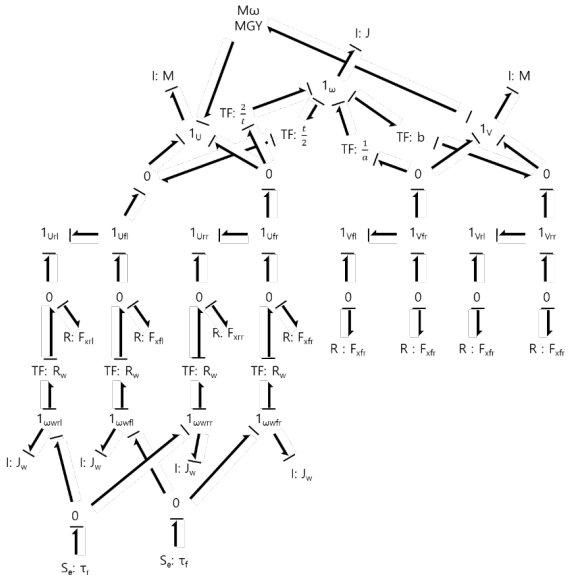

Figure 6: The bond graph for planar vehicle

Equations of motion are derived from above bond graph.

$$\dot{U} = \omega V + \frac{1}{M}\{F_{xfl} + F_{xfr} + F_{xrl} + F_{xrr} - (F_{yfl} + F_{yfr})\delta\}$$

$$\dot{V} = -\omega U + \frac{1}{M}\{F_{yfl} + F_{yfr} + F_{yrl} + F_{yrr} + (F_{xfl} + F_{xfr})\delta\}$$

$$\dot{\omega} = \frac{1}{J}\left\{a(F_{yfl} + F_{yfr}) - b(F_{yrl} + F_{yrr}) + \frac{t}{2}(F_{xfr} - F_{xfl} + F_{xrr} - F_{xrl})\right\}$$

$$\dot{\omega}_{ij} = \frac{1}{J_w}(\tau_i - R_w F_{xij})$$

$$i = front, rear, j = left, right$$

3 HANDLING SIMULATION AND RESULT

When the driver turns the steering wheel, the vehicle will change its direction. However, the characteristics of the tires and vehicle can affect how the vehicle moves, sometimes in an unexpected way. When a vehicle turns less than expected, it is called induced understeer. If a vehicle turns more than expected, it is called induced oversteer. Most of the produced vehicles have an understeer tendency. This understeer tendency usually becomes bigger and bigger with greater longitudinal velocity and greater steering angle.

On the other hand, literature shows that vehicles can have different steering tendencies as the drive torque distribution is changed (Klomp, Matthijs, and Robert Thomson 2011). Vehicles with traction torques on the rear wheels have larger yaw rates compared to vehicles driven by the front wheels, for similar levels of vehicle speed. As F_x is increased or decreased, the tire characteristic makes this change.

The actual meaning of understeer is rather complicate. Yaw rate is one of the dominant indicators which affect understeer. Therefore, yaw rate is used as the variable which decide the understeer in this paper. Yaw rate data from the planar vehicle model with a linear tire model is considered as the nominal yaw rate response. If the yaw rate output is lower than this, this paper refers to this as understeer. Figure 7 shows an example of that difference of yaw rate magnitude with respect to the drive axles types at 500Nm traction torque.

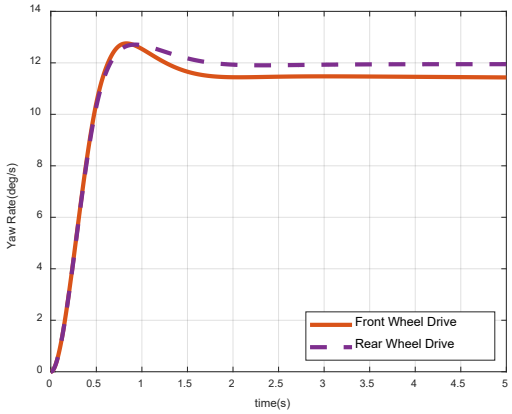

Figure 7: Difference of Yaw rate with respect to torque distribution

This paper simulates the planar vehicle model which has two traction motor to investigate the steering tendency with respect to various drive torque distributions. Furthermore, this torque distribution is simulated with not only traction torques but also regeneration torques which is a major advantage of the electric motor powertrain system, allowing for less understeer at the same speed.

The results are simulated with U = 80kph and with the parameters given in the appendix.

The steering input applied is 2 degrees on front wheels as shown in Figure 8. The total traction torque applied on front and rear axles are the same. Figure 10 shows how the total traction torque is distributed. The dotted line represents rear wheel drive vehicle. The total traction applied on only the rear axle. There is no traction torque on the front axle. On the other hand, the dashed line shows the motor torque of torque distribution control vehicle which is applied on front and rear opposite side. The total traction is similar at 200Nm. But the front has regenerative torque at -1100Nm. The rear has a traction torque of 1300Nm.

Figure 9. shows that vehicle driven only with rear wheel (dot), it has less yaw rate than nominal yaw rate(line). However, vehicle with distributed torque on front and rear opposite side (dash), shows similar levels of yaw rate compared with the nominal yaw rate. This indicates that motor traction control could make the vehicle have less understeer tendency.

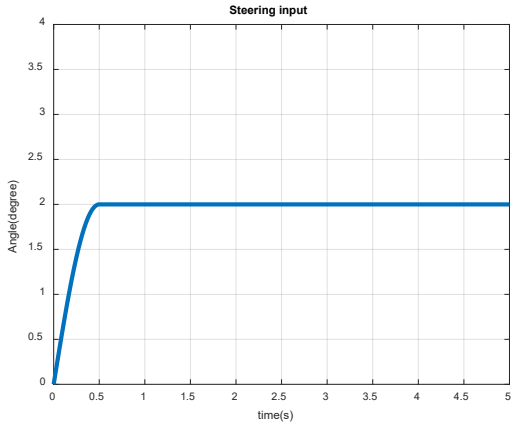

Figure 8: Steering input angle on Front wheel

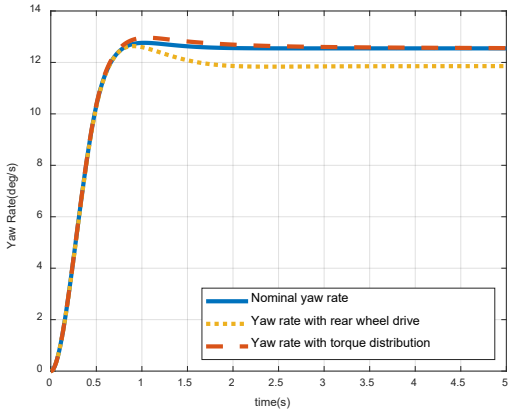

Figure 9: Yaw rate of the vehicle

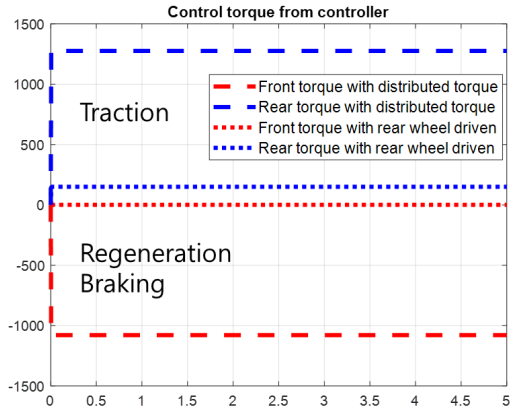

Figure 10: Traction and regeneration braking torque of front and rear motor

4 CONCLUSION

This paper presents a model of the planar vehicle with two traction motors, one on the front and one on the rear for simulating a handling maneuver. The simulation results show that the vehicle steer tendency is changed as torque distribution is changed. The results also can be controlled with appropriate torque distribution control. Further research will study the torque distribution controller with this model..

A APPENDICES

parameters	Description	Values
a	Length from C.G to front axle [m]	1.44

b	Length from C.G to rear axle [m]	1.56
t	Track width of the vehicle [m]	1.64
M	Mass of the vehicle [kg]	2,250
J	Moment of the inertia of the vehicle [kg·m^2]	3,445
g	Gravity [m/s^2]	9.81
R_w	Radius of the wheel [m]	0.33
J_w	Moment of the inertia of the wheel [kg·m^2]	1.7
H_{cg}	Height of the vehicle mass center	0.51
k_{rf}	Front roll stiffness of the vehicle	1,185
k_{rr}	Rear roll stiffness of the vehicle	932
C_x	Stiffness of the longitudinal tire force	105,000
C_α	Stiffness of the lateral tire force	40,800

.

REFERENCES

Osborn, R.P. and Shim, T., 2006. "Independent control of all-wheel-drive torque distribution." Vehicle system dynamics, 44(7), pp.529-546.

De Novellis, L., Sorniotti, A. and Gruber, P., 2013. "Optimal wheel torque distribution for a four-wheel-drive fully electric vehicle. SAE International Journal of Passenger Cars-Mechanical Systems," 6(2013-01-0673), pp.128-136.

De Novellis, L., Sorniotti, A. and Gruber, P., 2013. "Wheel torque distribution criteria for electric vehicles with torque-vectoring differentials." IEEE Transactions on Vehicular Technology, 63(4), pp.1593-1602.

Dugoff, H., Fancher, P.S. and Segel, L., 1970. "An analysis of tire traction properties and their influence on vehicle dynamic performance." SAE transactions, pp.1219-1243.

Margolis, D.L. and Asgari, J., 1991. "Multipurpose models of vehicle dynamics for controller design" (No. 911927). SAE Technical Paper.

Klomp, M. and Thomson, R., 2011. "Influence of front/rear drive force distribution on the lateral grip and understeer of all-wheel drive vehicles." International journal of vehicle design, 56(1-4), pp.34-48.

AUTHOR BIOGRAPHIES

DONGHUN LEE is a vehicle test engineer at Hyundai motor company. His research interests in vehicle chassis control for handling and braking. His email address is a.dhoonil@hyundai.com.

JONATHAN LOYOLA is a Ph.D. candidate and a graduate student researcher working at the Hyundai Center of Excellence in Vehicle Dynamic Systems & Control located at the University of California, Davis. He holds a master's degree from Davis in mechanical engineering. His research interests lie in system modeling, vehicle dynamics, and controls. His email address is jonloyola@ucdavis.edu.

JORDAN MCCRONE is a graduate student researcher in the Hyundai Center of Excellence at UC Davis, a collaborative venture between student and faculty at UC Davis and visiting engineers from Hyundai in Korea. His research interest is in vehicle dynamics modeling and control. His email is djmccrone@ucdavis.edu.

DONALD L. MARGOLIS is a professor of mechanical engineering and director of the Hyundai Center of Excellence in Vehicle Dynamics Systems & Control at UC Davis. He has extensive experience in teaching system dynamics at the graduate and undergraduate levels, consultation in vibration controls, and has published numerous papers on the industrial applications of dynamics. His email is dlmargolis@ucdavis.edu.